МІНЕРАЛОГІЯ, ГЕОХІМІЯ ТА ПЕТРОГРАФІЯ

УДК 550.8+549.6+550.4+550.8

S. Shnyukov, Dr. Sci. (Geol.), Assoc. Prof.
E-mail: shnyukov@mail.univ.kiev.ua
I. Lazareva, Cand. Sci. (Geol.), Assoc. Prof.
E-mail: lazareva@mail.univ.kiev.ua
O. Zinchenko, Cand. Sci. (Geol.), Assoc. Prof.
E. Khlon, Engineer
E-mail: khlon@univ.kiev.ua
L. Gavryliv, PhD student
E-mail: liubomyr.gavryliv@gmail.com
A. Aleksieienko, PhD student
E-mail: scr315@gmail.com
Taras Schevchenko National University of Kyiv
Institute of Geology, 90 Vasylkivska Str., Kyiv, 03022, Ukraine

GEOCHEMICAL MODEL OF PRECAMBRIAN GRANITOID MAGMATIC EVOLUTION IN THE KOROSTEN PLUTON (UKRAINIAN SHIELD): PETROGENETIC ASPECTS AND GENESIS OF COMPLEX ORE MINERALIZATION IN METASOMATIC ZONES

(Рекомендовано членом редакційної колегії д-ром геол. наук, проф. О.В. Митрохиним)

Preliminary geochemical dataset for the granitoids (rapakivi, granite-porphyries, veined granites) of Korosten anorthosite-rapakivi granite pluton (Ukrainian Shield) was studied. The data set includes the results of all major and selected trace elements determinations (XRF, >300 samples), and is compared with melt crystallization and partial melting models of trace elements behavior. Only the Rayleigh model closely approximates the trace element data for granitoids. Typical incompatible behavior under approximately constant bulk distribution coefficient is determined for Rb (D_{Rb} = 0,5). Model f values (weight fraction of liquid in magma chamber) are calculated for each granitoid type (residual melt portion) from Rayleigh equation and Rb content in rocks (C_{Rb}) assuming minimum concentration in granitoids (169 ppm) as Rb content in parent magma (C_0^{Rb}). C vs. f curves for trace (including P, Ti, S, Cl, F, Ca) and major elements are approximated by means of equations of $C=C_0?f^{D-1}$ form or polynomial ones respectively. This set of equations is an idealized model of element behavior that demonstrates the depletion of Ba, Sr, Ti, Zr, P, S and enrichment of Th and Ga in the residual liquid as well as the inversion behavior of LREE, Y, F, Cl, Nb, Zn and Pb during the melt fractional crystallization in magma chamber. Monotonous decrease of both Zr and P content indicates melt saturation in zircon and apatite. Therefore, model temperature (T_{model}) of the melt is estimated from equations of zircon and apatite solubility. The temperature evolution in magma chamber was presented as T_{model} vs. f polynomial equation (T_{model} range: 900-720°C). Inversion in LREE content (f = 0,185) indicates the apatite/monazite replacement in the crystallizing assemblage. Water content in melt for this f value and corresponding T_{model} was calculated from equation of monazite solubility which demonstrates its high H_2O-dependence. C_0^{H2O}=2,36 wt% was estimated on this basis (assuming D_{H2O} = 0,1) for the liquidus of initial granite melt (P_{total} ~6,3 kbar). According to designed model water saturation limit was reached at f = 0,165 and H_2O-fluid was extracted from the melt during its further evolution. Synchronous inversion of C/C_0 vs. f curves shows the enrichment of fluid with F, Cl, Nb, Zn, Pb etc. Such characteristics of fluid are in agreement with geochemical data for ore-bearing altered rocks and might testify for their genetic unity.

Keywords: granite, rapakivi, trace element, magmatic evolution, apatite, zircon, monazite, xenotime, solubility, water in melt, fluid extraction, altered rocks, ore mineralization.

Introduction. Korosten pluton (KP) is one of the largest and best studied magmatic complexes of Ukrainian Shield (USh). It occupies the northwestern part of it and covers an area of approximately 12000 km^2 [21, 54]. Pluton (fig. 1) comprises typical anorthosite-rapakivi granite association (ARGA) and represents complex multistage intrusive body with at least 50 Ma of emplacement history (≈1,8-1,75 Ga [6, 8, 28, 39]). Three main groups of rocks are distinguished at present erosional level: granitoids and related pegmatites (4 bodies that cover 75% of KP); gabbroids (3 large bodies); hybrid rocks, which formed as a result of gabbroic and granitic magma mixing according to [33]. Gabbroid and granitoid bodies themselves represent polyphase intrusions composed by rocks associations of different age [6, 10, 19, 20, 54 etc.]. Two anorthositic (A1, A2) and two gabbroic (G3, G4) phases are distinguished among the gabbroids, the earliest phase (A1) age is estimated as 1,8-1,784 Ga and later phases are believed to be 1,763-1,758 Ga [6, 33, 39, 54]. Three phases of granitic intrusions are confirmed for the KP [9, 18, 22, 27, 31]: γ^1 – rapakivi granites and biotite-amphibole rapakivi-like granites, γ^2 – subalkali biotite leucogranites and granite-porphyries, γ^3 – vein rare-metal microgranites and granite-porphyries, which are dated as 1767±5, 1752±16, 1737±54 Ma respectively [22, 33]. Age of gabbro-monzonites and granosyenites (hybrid rocks) is estimated as 1760,7±4,1 and 1763,8±2,6 Ma respectively [33].

Long history of KP research [1, 5-16, 18, 20-25, 27, 28, 31-36, 39, 43, 54 etc.] led to formation of ***two major models*** of its formation. ***First model*** [1, 4 et al.] accepts fractional crystallization of basic melt as leading mechanism of all rocks formation (especially granitic and gabbroic components). Model stands on the basis of evident spatial association of granitoids and gabbroids with hybrid rocks as transitional link as well as experimentally proved [51 etc.] possibility of such scenario. Nevertheless, the model poorly describes aforementioned datings and dominating position of granitic rocks in KP. ***Second model*** implies bimodal magmatism and lacks direct genetic relations between granitoids and gabbroids [5, 23 etc.]. Model suggests partial melting of granulitic substratum under the influence of mantle melts as main mechanism, which resulted in formation of peraluminous melts due to mixing of mantle and lower crust material. Basic rocks formation was initiated by intrusion of such melts in higher crust levels that was followed by formation of transitional chambers and differentiation in them. Granitoids are believed to be formed as a result of middle level crust melting by high-temperature basic magmas [21, 23 etc.]. Objective analysis points out that second model is better grounded and is also proved by data on deep crustal structure of northwestern part of USh obtained by a complex of modern geophysical methods modeling [14, 16, 54 etc.].

Therefore, conducted geological, petrologic and geophysical research allowed to suggest realistic models of KP formation and to assess conditions of leading rock types crystallization. According to mineral thermobarometry data [21], crystallization of A1 type anorthosites took place under ~1000°C temperature and depth of ~30 km or more. Similar

data on A2 type anorthosites yields temperature of 800-850°C and depth of ~18 km [21]. As for prevailing granites, mineral thermobarometry [1, 23] and fluid inclusions study [7, 13, 15, 25] suggests a wide range of depths (3 to 12 km) and temperatures (850-600°C for granitoids and 600-350°C for pegmatites) of crystallization, which corresponds to upper continental crust level. However, introduced models [1, 4, 5, 14, 23, 54 etc.] suggest generation and subsequent differentiation of ***granitic melts*** in much deeper conditions. ***The problem*** is that mechanisms and conditions of such processes are insufficiently studied.

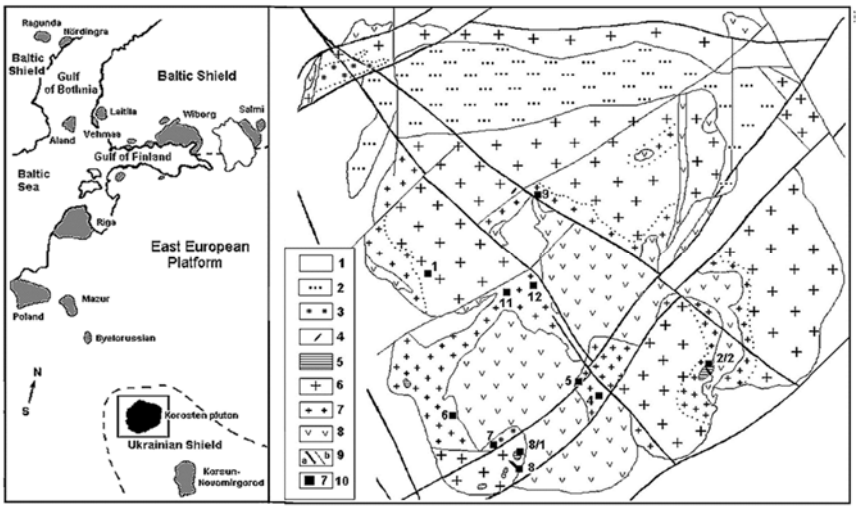

Fig. 1. Geological position and structure of Korosten Pluton. (a) Position of the Korosten pluton in the East European platform (after [1]). (b) Simplified geological map of Korosten Pluton [11, 27, 43], with this paper author's modifications:
1 – Early Proterozoic gneisses, migmatites, granites; 2 – sedimentary-volcanic rocks of the Ovruch group; 3 – altered rocks in tectonic zones (I – Suschano-Perga zone; II – Teterev zone); 4 – rare-metal granite dykes; 5 – granite porphyry; 6 – porphyritic coarse-grained rapakivi granites with minor ovoides (Amph+Bt, Bt); 7 – rapakivi granites with micro to large size ovoids (Amph+Bt±Px±Ol); 8 – anorthosites, gabbro-norites, gabbro-diabases. 9 – faults (a–regional, b–local); 10 – sampling locations with their numbers

In present paper authors make an attempt to solve the latter problem at an example of KP granitoid series by means of representative set of geochemical data complex analysis. Reaching the aim requires solving next tasks: (1) development of KP granitoids evolution geochemical model, (2) model evaluation of thermodynamic parameters and fluid mode of magma chamber evolution (3) assessment of granitic magma potential to generate high-temperature ore-bearing fluids able to large-scale metasomatic alteration of host rocks and mineral deposits formation.

Sampling and analytical techniques. All the granitic rocks of the Korosten pluton, taking into account the results of this paper as well as early published ones [12, 18, 20, 27, 31, 43 etc.] are classified into 11 main varieties (types) of rocks that are widely distributed all over the pluton. Each type is investigated in details, while main rock types constitute a simplified but a representative description of trace and major elements abundance variations within the Korosten pluton granitoids.

Locations of sampling with their numbers are shown in Fig 1. All the sampled types of rocks, with short description, are listed below (see Table 1) in an order of *f* parameter values reduction. A decrease of *f* parameter value obtained as a result of geochemical modelling is in correlation with the rock types relative emplacement ages. Each rock type is investigated by a number of ordinary point samples (n=19–25) to carry out element analysis and one bulk representative sample to make a detailed geochemical and mineralogical analysis. Bulk representative samples are additionally studied through thin sections and heavy mineral concentrates to establish complete mineralogical composition. The presence of trace amounts (up to separate grains concentration level) of accessory phases of zircon-apatite-monazite-xenotime association is checked during the research. Mineralogical investigation results are summarized in a concise description of rock types added to the Table 1.

Both ordinary and bulk representative samples are crushed, pulverized and analyzed by means of quantitative X-ray fluorescence method (XRF) at the laboratory of Institute of Geology, Taras Shevchenko National University of Kyiv, Ukraine. Major oxides and selected trace elements (SiO_2, TiO_2, Al_2O_3, $Fe_2O_3^{total}$, MnO, MgO, CaO, Na_2O, K_2O, P_2O_5, S, Cl, Zr, Sr, Ba, Rb, Y, La, Ce, Nd, Nb, Th, Ga, Pb, Zn, Cu) are analyzed in each sample. The precision and accuracy of XRF method is verified by a replicate analysis of the rock standards of specially prepared reference samples set. Final calculations for each powdered sample are obtained as averages of individual powder pellets analysis with 3-5 measurements in case of point samples and 10-30 measurements in case of bulk ones. Thus, all 315 final calculations represent averages of more than 1500 analyses of powder pellets.

The latter analytical procedure made it possible to minimize analytical uncertainties that may arise in case of non-homogenous trace elements distribution in powdered samples. The best results (decreased n-fold) are obtained for P, LREE (La, Ce, Nd) and especially for Zr – the elements that form their own accessory phases of apatite, monazite and zircon. For all bulk samples total analytical uncertainty with a confidence level of 95% is estimated to be (in relative %): Si – 0.5-0.6%; Al, Fe, Na, K, Rb, Ba – 1.5-5%; Ti, Mn, Mg, Ca, P, Zr, Sr, Y, La, Ce, Nd – 5-10%; Nb, Pb, Th, Cu, Zn, Ga – 10-15% (up to 20-40% for ~20 ppm level); S, Cl – 15-30%. In case of point samples noticeable analytical uncertainty is noticed only for Zr (up to 15-25%). Other elements show lesser uncertainties (P, LREE etc.) or insignificant ones (major elements).

Representative whole-rock data set used for geochemical modelling is formed on the basis of analytical results. Each Korosten granitoids rock type includes (1) compositions calculated as averages of point samples analyses (see Table 3); (2) the composition of bulk (see Table 2) samples (22 whole-rock analyses in total). Representative data for F average content in rock types [27] is added to this set. Geochemical data set for altered rocks includes only the ordinary samples analyses.

Table 1

Localities and modal mineralogical composition of investigated granite types

Sample (rock type) No (No on Fig. 1)	f range	Rock type, locality	Rock-forming and accessory minerals content (vol. %)							Zr-P-LREE-Y accessory minerals association
			Fsp	Pl	Qtz	Hbl	Bt	Ol+Px	Acc	
95004 (4)	0,784-0,995	Rapakivi granite, village Mirnoye	48	18	21	7	3.5	0,5	2	Zrn+Ap
95006 (6)	0,875-0,877	Rapakivi granite, Volynsk pegmatite field	49	22	20	4,5	3	0,3	1,2	Zrn+Ap
95002/2 (2/2)	0,613-0,865	Rapakivi granite, town Malyn	45	21	20	8,5	3	0,3	2,2	Zrn+Ap
95005 (5)	0,721-0,734	Rapakivi granite, village Guta Potievka	54	14	24	4	1	n.d.	3	Zrn+Ap
95012 (12)	0,520-0,580	Rapakivi granite, town Korosten	51	8	34	2	1,5	0,1	3,4	Zrn+Ap
95011 (11)	0,406-0,426	Granite, village Schorsovka	59	7	29	0.9	1,2	0,4	2,5	Zrn+Ap
95009 (9)	0,347-0,408	Granite, village Ignatpol	48	16	30	1	3,5	n.d.	1,5	Zrn+Ap
96001 (1)	0,382-0,401	Granite, village Emelyanovka	50	15	29	1,5	3	n.d.	1,5	Zrn+Ap
95008/1 (8/1)	0,199-0,251	Granite-porphyry, village Andreevka	54	12	23	0,5	7	n.d.	3,5	Zrn+Ap+Mnz
95007 (7)	0,124-0,194	Autometamorphic granite, village Lezniky	52	14	28	1	3**	n.d.	2	Zrn+Mnz+Xnt
95008 (8)	0,029-0,038	Veined rare-metal granite, village Andreevka	31	28*	31	n.d.	7.5***	n.d.	2,5****	Zrn±Xnt

Notes: Fsp – K-feldspar, Pl – plagioclase (* albite), Qtz – quartz, Hbl – hornblende, Bt – biotite (** Li- biotite, *** zinnwaldite), Px+Ol – pyroxene+olivine (relic), Acc – accessory minerals (**** including ≤2.5% topaz and ≤0.1% other accessories), Zrn – zircon, Ap – apatite, Mnz – monazite, Xnt – xenotime; n.d. – not detected.

Modelling procedure and results.

Model options. Five idealized models of trace elements behaviour during melt crystallization and partial melting are suitable for geochemical modelling of real magmatic processes [29, 30, 38, 41, 44, 46, 50, 52 etc.]. These models, simplified for the case of constant bulk distribution coefficient, are presented below by equations (1) (Rayleigh fractional crystallization), (2) (equilibrium melt crystallization and batch melting), (3) (fractional partial melting with melt accumulation in magma chamber) and (4) (strict fractional partial melting):

$$C = C_0 \cdot f^{D-1}, \quad (1)$$

$$C = C_0 \cdot \left[D \cdot (1-f) + f\right]^{-1}$$

and

$$C = C_0^S \cdot \left[D \cdot (1-f) + f\right]^{-1}, \quad (2)$$

$$C = \left(C_0^S / f\right) \cdot \left[1 - (1-f)^{1/D}\right], \quad (3)$$

$$C = \left(C_0^S / D\right) \cdot (1-f)^{(1/D)-1}, \quad (4)$$

where C is the element concentration in the melt, C_0 and C_0^S – initial element concentration in the parent melt and parent solid rock respectively, D – bulk distribution coefficient for the element, f – weight fraction of liquid (melt) in the system.

To apply the general forms of these equations [44, 46] the value of D variations (dependent on the temperature, pressure, melt and solid phase composition) during magma evolution should be obtained. Due to absence of the latter data in practice, only simplified equations could be used in geochemical modelling. Generally, the models, designed on this base, are semiquantitative, but they demonstrate close approximation to magmatic evolution if D values for some compatible and (or) incompatible elements are approximately constant and might be determined.

Granitoids magmatic evolution is a typical example in this case. The temperature range and variations in melt and solid phase composition of granite-forming systems are less studied than those of basalt-forming ones. Therefore, approximately constant *D* values could be calculated for the elements with the distributional pattern controlled only by main rock-forming minerals. Rb and Sr are the typical elements of this group. According to the data available [2, 30], a set of *D* values may be suggested to be used in geochemical modelling of such typical geological environments: (1) melt crystallization with K-feldspar and plagioclase as the main phases of the crystallizing assemblage (D_{Rb}=0.5, D_{Sr}=2), (2) partial melting at lower crustal level with plagioclase as the main restite phase (D_{Rb}=0.1, D_{Sr}=2). In case of partial melting at the upper mantle level (olivine and pyroxene as the main restite phases), D_{Rb}=0.1 and D_{Sr}=0.1 values are the most realistic estimations obtained. The latter set of *D* values is used in further modelling procedure.

The data available confirms contrary role (compatible and incompatible) of Rb and Sr (as well as Ba) during the formation of Korosten pluton granitoids (Fig. 2, a). Therefore, our data set for the Korosten pluton and the data sets of other granitoids complexes of the Ukrainian Shield [9], obtained by means of XRF and reported by [10, 12], were studied in comparison with the different model trends of melt crystallization and partial melting in order to choose between different models for the Korosten granitoid complex (Fig. 3, a). Model trends calculated are based on equations (1) – (4) assuming suggested D_{Sr} and D_{Rb} values (vide supra) for *f* that varies from 1.0 to 0.01. Both trends and granitoids data are plotted in Sr_{max}/Sr_{min}–Rb_{max}/Rb_{min} coordinates, where Sr_{max}, Rb_{max} and Sr_{min}, Rb_{min} are the elements maximum and minimum concentrations within the granitoids series for each complex or pluton. Only Rayleigh model (1), which is the most applicable for the granitoids [17, 23, 30] represents melt crystallization process on this plot. Other models (2) – (4) represent partial melting processes.

According to Fig. 3, a the Korosten pluton granitoids as well as all other granitoids complexes of the regions of Proterozoic activation and some complexes of gneiss-amphibolitic regions demonstrate a good agreement with Rayleigh model in case of D_{Rb}=0.5, D_{Sr}=2 (K-feldspar and plagioclase fractionation during the melt crystallization). Strong linear correlation (fig. 2, b) between the logarithms of Rb, Sr and Ba concentrations testify to the same result, as well as it shows the constant D_{Rb}, D_{Sr} and D_{Ba} values during the process of fractional crystallization. Coefficients values in a corresponding linear equation for Sr and Rb (fig. 2, b) confirm that D_{Rb}=0.5 and D_{Sr}=2 values are correct in a case of the Korosten pluton granitoids formation. Similar plot for all present data on Ukrainian Shield granitoids approximated to Rayleigh model (fig. 3, b) shows that these values are a good estimation in a general case too.

Table 2

Major and trace element composition of Korosten pluton main granitoids types (representative bulk samples)

Sample (rock type) No	95004	95006	95002/2	95005	95012	95011	95009	96001	95008/1	95007	95008
Major elements, wt%											
SiO_2	71,73	72,88	72,84	73,69	73,22	75,45	76,81	75,16	75,72	76,35	78,16
TiO_2	0,335	0,384	0,286	0,368	0,284	0,291	0,193	0,202	0,182	0,122	0,012
Al_2O_3	13,48	12,16	12,9	11,95	12,96	11,56	11,35	12,6	11,73	11,51	11,91
$Fe_2O_3^{total}$	3,46	3,642	3,19	3,491	2,81	2,685	1,97	2,06	2,44	2,06	0,929
MnO	0,045	0,049	0,042	0,039	0,039	0,037	0,033	0,033	0,03	0,027	0,032
MgO	0,134	0,147	0,134	0,196	0,233	0,138	0,107	0,104	0,079	0,056	0,039
CaO	1,639	1,476	1,445	1,142	1,03	0,945	0,63	0,766	0,888	0,853	0,074
Na_2O	3,229	3,484	3,264	3,152	3,53	3,003	3,08	3,36	3,39	3,49	4,61
K_2O	5,263	5,181	5,228	5,372	5,31	5,304	5,22	4,93	4,77	4,91	3,63
P_2O_5	0,098	0,09	0,067	0,098	0,069	0,052	0,026	0,029	0,026	0,012	0,024
S	0,084	0,064	0,072	0,112	0,056	0,069	0,057	0,05	0,046	0,046	0,032
Cl	0,023	0,011	0,02	0,028	0,01	0,01	0,01	0,01	0,034	0,028	0,002
F	0,078	0,08	0,04	0,06	0,145	0,059	0,12	0,16	0,213	0,3	0,371
LOI (~H_2O^+)	0,047	0,057	0,201	0,037	0,022	0,183	0,223	0,318	0,223	0,052	<0,01
Trace elements, ppm											
Cu	23	20	23	22	27	23	23	20	22	19	17
Zn	91	80	91	101	84	85	82	94	122	100	64
Ga	20	21	21	18	19	23	17	23	20	25	24
Rb	191	181	182	199	222	265	265	274	379	384	864
Sr	131	107	101	81	74	49	24	39	30	13	5
Y	46	41	49	48	57	54	48	67	121	176	58
Zr	645	511	482	572	555	405	304	360	380	316	140
Nb	31	25	29	28	33	25	25	36	42	45	45
Ba	1440	1130	877	833	929	574	222	318	217	35	20
Pb	27	27	44	34	33	35	31	27	49	51	50
Th	8	11	15	9	18	15	22	21	33	18	36
La	93	67	70	81	87	73	78	93	134	105	13
Ce	145	114	124	119	158	117	139	166	234	142	13
Nd	57	51	54	51	56	52	49	61	80	43	19
Weight fraction of liquid (melt) in the system											
f	0,784	0,876	0,865	0,721	0,579	0,406	0,408	0,382	0,199	0,193	0,038

Notes: $Fe_2O_3^{total}$ – all Fe as Fe_2O_3.

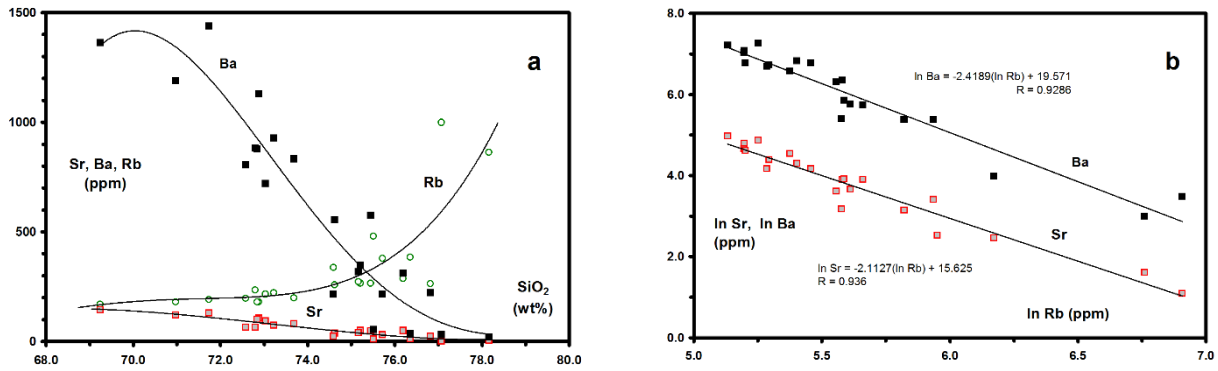

Fig. 2. Sr, Ba and Rb geochemistry in Korosten Pluton granitoids. (a) Elements concentration vs. SiO_2 content, (b) ln Sr and ln Ba as a linear functions of ln Rb

The opposite result was obtained for all granitoids complexes of the greenstone, gneiss-granulitic regions and some complexes of gneiss-amphibolitic regions of Ukrainian Shield [9]. As it is seen at Fig. 3, a the data of these complexes is in a good agreement with (2) and (3) partial melting models. According to the preliminary results of semiquantitative modelling (fig. 3, b) the granitoids of these complexes were presumably formed during the partial melting of plagioclase-bearing lower crust originally derived from mantle. Their crustal Sr and Nd isotopic composition, reported by [3, 11, 32, 43 etc.] confirms this assumption.

Major and trace elements behavior during magma evolution. Model *f* values for each granitoid type (residual melt portion) are calculated from Rayleigh equation (1), Rb content in rocks (C_{Rb}) assuming K_{Rb}=0.5 and a minimum Rb abundance for all Korosten granitoids series (169 ppm) as initial Rb content in the parent magma (C_0^{Rb}):

$$f = \left(C/C_0\right)^{1/(D-1)} = \left(169/C_{Rb}\right)^2. \quad (5)$$

All trace elements (including P, Ti, S, Cl, F, CaO) and major oxides (including M and D bulk composition parameters explained in the next paragraphs) are plotted against *f* (fig. 4-6) and approximated by means of equations of $C = C_0 \cdot f^{D-1}$ type or polynomial ones respectively. Only some major elements data for autometamorphic rocks (especially shown in Fig. 6, a, 6, c and 6, d) are excluded from the approximation.

In such a way, geochemical data set is transformed in a set of model equations (presented in Fig. 4-6), which contains the information about *D* and C_0 (ppm) values for all determined trace elements. This set is an idealized model

of elements behavior during the melt fractional crystallization in magma chamber.

Idealized C vs. *f* plots (fig. 4, 5 and 6, a) demonstrate the monotonous decrease of Ba, Sr, S, Ti, Zr, CaO concentrations as well as P (almost over the whole range of *f* values) and the monotonous increase of Th and Ga in the residual liquid caused in both cases by their approximately constant bulk distribution coefficients (stable composition of the crystallizing assemblage). Some elements (LREE=La+Ce+Nd, Y, F, Cl, Nb, Zn and Pb) demonstrate inverse behavior – their contents increase at first and then decrease later during crystallization or vice versa. The latter behavior can be explained by two processes: (1) the appearance of new accessory minerals in the crystallizing assemblage or (and) (2) metal-bearing fluid extraction from the melt.

Table 3

Major and trace element average composition of Korosten pluton main granitoids types (ordinary point samples)

Sample (rock type) No	95004	95006	95002/2	95005	95012	95011	95009	96001	95008/1	95007	95008
Major elements, wt%											
SiO_2	69,24	70,97	73,03	72,58	72,80	74,62	76,19	75,21	74,59	75,51	77,07
TiO_2	0,368	0,442	0,283	0,369	0,349	0,278	0,223	0,167	0,185	0,137	0,018
Al_2O_3	14,29	13,26	12,77	12,74	12,22	12,50	11,85	12,52	12,65	11,79	12,87
$Fe_2O_3^{total}$	4,08	4,27	3,26	3,61	3,58	2,55	2,31	2,16	2,27	2,61	0,92
MnO	0,049	0,060	0,045	0,047	0,043	0,043	0,042	0,029	0,03	0,027	0,037
MgO	0,171	0,178	0,133	0,173	0,231	0,135	0,128	0,105	0,092	0,052	0,038
CaO	1,991	1,586	1,322	1,281	1,114	0,975	0,5	0,88	0,772	0,9	0,084
Na_2O	3,47	3,39	3,29	3,26	3,46	3,19	3,01	3,415	3,45	3,38	4,96
K_2O	5,59	5,24	5,28	5,35	5,49	5,27	5,13	5,14	5,18	5,06	3,46
P_2O_5	0,097	0,11	0,054	0,101	0,072	0,043	0,039	0,027	0,027	0,009	0,023
S	0,204	0,044	0,067	0,043	0,019	0,018	0,046	0,03	0,034	0,019	0,017
Cl	0,022	0,007	0,023	0,008	0,002	0,006	0,007	0,009	0,019	0,01	0,002
F	0,078	0,08	0,04	0,06	0,145	0,059	0,12	0,16	0,213	0,3	0,347
LOI (~H_2O+)	0,04	0,096	0,146	0,17	0,118	0,102	0,223	0,022	0,287	0,027	<0,01
Trace elements, ppm											
Cu	n.a.	n.a.	33	n.a.	n.a.	n.a.	23	n.a.	n.a.	n.a.	n.a.
Zn	n.a.	n.a.	103	n.a.	n.a.	n.a.	81	n.a.	n.a.	n.a.	n.a.
Ga	n.a.	n.a.	20	n.a.	n.a.	n.a.	19	n.a.	n.a.	n.a.	n.a.
Rb	169	181	216	197	234	259	287	267	338	479	1000
Sr	145	121	95	65	64	37	50	50	23	12	3
Y	48	40	63	38	45	43	49	50	125	136	74
Zr	498	489	475	424	530	415	317	249	348	363	129
Nb	24	19	31	19	22	10	30	22	31	59	29
Ba	1363	1189	720	805	883	554	311	349	216	54	33
La	100	70	95	73	105	92	60	84	200	133	27
Ce	180	127	184	124	181	144	116	132	315	197	47
Nd	81	61	90	57	71	59	60	47	119	59	10
Pb	n.a.	n.a.	30	n.a.	n.a.	n.a.	32	n.a.	n.a.	n.a.	n.a.
Th	n.a.	n.a.	16	n.a.	n.a.	n.a.	19	n.a.	n.a.	n.a.	n.a.
Number of samples											
N	20	19	20	21	20	25	20	20	20	19	20

Notes: $Fe_2O_3^{total}$ – all Fe as Fe_2O_3, n.a. – not analyzed.

Accessory minerals crystallization and estimation of the melt temperature. Monotonous decrease of Zr content (fig. 4, b, 7, a) indicates the saturation of the residual melt in zircon over the whole observed range of *f* values (*f*=1-0.01). The data on P content demonstrate more complicated situation. Hence, similar monotonous decrease of P content as well as saturation of the residual melt in apatite is noticed only for *f* values lying within the range of 1-0.185 (fig. 4, a, 7, a). According to model C vs. *f* plots and modal mineralogical composition of the investigated rock types (fig. 7, a, 7, b), inversion in LREE and Y content indicates the change of apatite to monazite and monazite to xenotime in the crystallizing accessory minerals assemblage. The most important parameters of the apatite/monazite replacement point are presented on Fig. 7.

In any cases, monotonous decrease of Zr and P content indicates saturation of the residual melt in both zircon and apatite over a wide range of *f* values (1-0.185). Therefore, temperature of the melt in magma chamber at moment of each residual melt portion (granitoids rock type) extraction is calculated using experimentally determined [45, 56] zircon (6) and apatite (7) solubility equations on a basis of melt composition obtained for Zr (ppm), P (ppm), M and D from the designed model equations (fig. 4 and 6):

$$\ln D_{Zr}^{Zrc/L} = \left[-3{,}80\text{-}0{,}85\cdot(M\text{-}1)\right] + 12900\cdot T^{-1}, \quad (6)$$

$$\ln D_{P}^{Apt/L} = \left[-3{,}1 - 12{,}4\cdot(SiO_2\text{-}0{,}5)\right] + \left[8400 + 26400\cdot(SiO_2\text{-}0{,}5)\right]\cdot T^{-1}, \quad (7)$$

where $D_{Zr}^{Zrc/L} = Zr^{Zrc}/Zr^{L}$, $D_{P}^{Apt/L} = P^{Apt}/P^{L}$ and Zr^{Zrc}, P^{Apt}, Zr^{L}, P^{L} – Zr and P content (ppm, wt%) in stoichiometric zircon, apatite and melt respectively, P^{Apt}

$M = \frac{Na+K+2Ca}{Al\cdot Si}$ (cation ratio of the melt), SiO_2 – weight fraction of silica in the melt, T – absolute temperature (^{0}K). T_{Zr} and T_P are the temperatures calculated from the equations (6) and (7) respectively. T_{model} is an average of T_{Zr} and T_P in a range of *f* from 1 to 0.185 and extrapolated to *f* = 0.02. T_{model} during the fractional crystallization within the estimated range of 900-720°C is presented in Fig. 7, c as T_{model} vs. *f* polynomial equation. According to this equation, T_{model} value for apatite/monazite replacement point is estimated to be 825 20 °C (fig. 7, c).

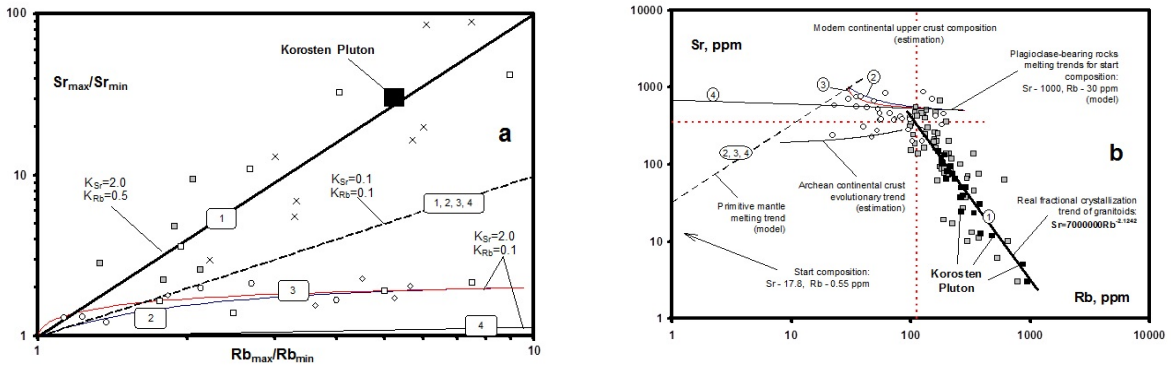

Fig. 3. Comparison of the data on Korosten Pluton and other granitoids of Ukrainian Shield with the model trends of melt crystallization and partial melting. (a) Open circles, rhombs and squares – granitoid complexes of greenstone, gneiss-granulitic and gneiss-amphibolitic regions respectively; full squares – granitoid complexes of the regions of Proterozoic activation; crosses – some typical differentiated complexes of the Earth [5]. (b) Full squares – Rayleigh model (1) approximated granitoid complexes. All estimations of Earth mantle and crust trace element composition are taken from [50]. See text for references and description of models (numbers in circles) and modelling procedure

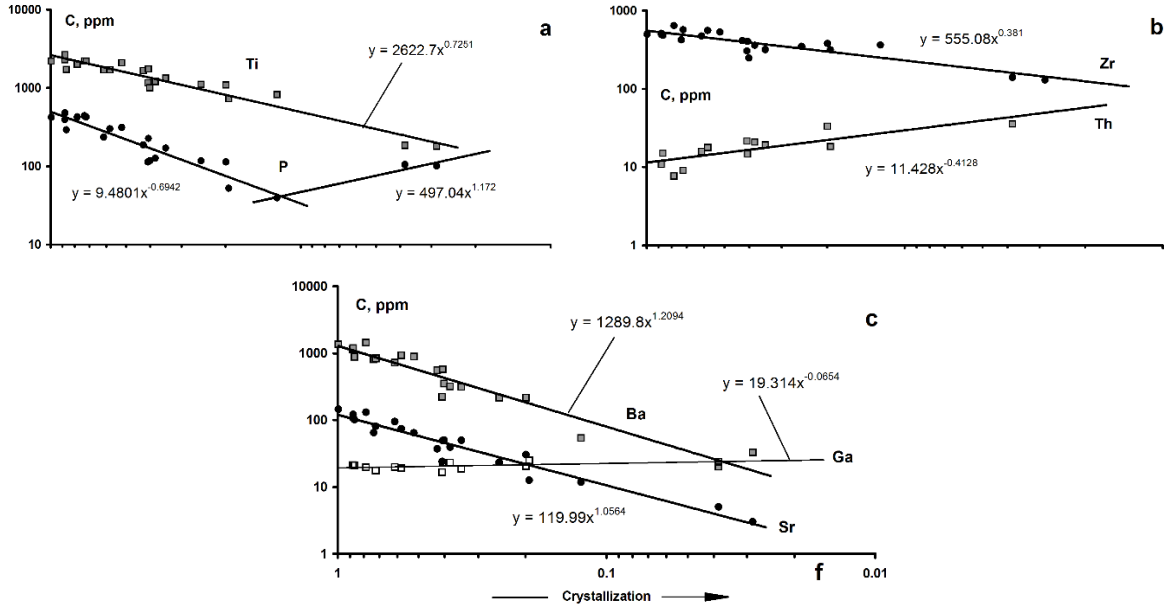

Fig. 4. P, Zr, Ti, Th, Ba, Sr, Ga concentrations in Korosten pluton granitoids vs. f

Estimation of water content in melt, liquidus point total pressure and the conditions of water-fluid extraction from the melt. The residual melt in apatite/monazite replacement point is characterized by saturation in both apatite and monazite accessory phases. Therefore, the occurrence of this replacement within the Korosten pluton granitoids evolution creates the possibility for water content estimation in melt under the certain conditions for this replacement point (fig. 7). For reaching the goal, a monazite solubility equation (8) which demonstrates a high H_2O-dependence of monazite solubility [49] is used:

$$\ln REE^{L} = 9{,}50 + 2{,}34 \cdot D + 0{,}3879 \cdot (H_2O)^{0{,}5} - 13318 \cdot T^{-1}, \quad (8)$$

where REE^{L} – LREE (La-Gd, excluding Eu) concentration (divided by atomic weight) in the melt, $D = \frac{Na+K+Li+2Ca}{Al \cdot (Al+Si)}$ (cation ratio of the melt), H_2O – water content in the melt (wt%), T – absolute temperature (K).

As a result, C_{H2O} in apatite/monazite replacement point (f=0.185, T_{model}=825 °C, D=1.148, LREE=404.6 ppm) is estimated to be 10.77 wt% (fig. 8, a). $C_0^{H_2O}$ is calculated from the equation (1) assuming D_{H20}=0.1 and it equals 12.36 wt%. The latter water content at the liquidus of initial granite melt corresponds to total pressure (P_{total}) of approximately 6.3 kbar [30, 47].

According to Rayleigh equation (1) for the conditions of the designed model ($C_0^{H_2O}$ = 2.36 wt%, D_{H20}=0.1) and assuming both approximate temperature dependence on water solubility in albite melt [48] and water solubility in granite melt under P_{total}=6.3 kbar reported by [30, 47], water saturation limit was reached at f=0.165 (fig. 8, a). After this moment H_2O-fluid was extracted from the melt during its further evolution.

Water-fluid composition and its comparison with composition of altered rocks. The beginning of water-fluid extraction from the melt (f=0.165) and f values estimated for model C/C_0 vs. f plots inversions are almost synchronous for F and Cl as well as for such typical polymetallic and rare elements as Zn, Pb and Nb (fig. 8, b). The latter phenomenon testifies to high F and Cl content in extracted H_2O-fluid and shows its enrichment in these elements. Such characteristics of extracted fluid as well as expected high Rb and low Sr and Ba content are in agreement with geochemical data obtained for ore-bearing altered rocks from metasomatic zones associated with Korosten pluton [19, 24, 36 etc.] and testify to their genetic unity.

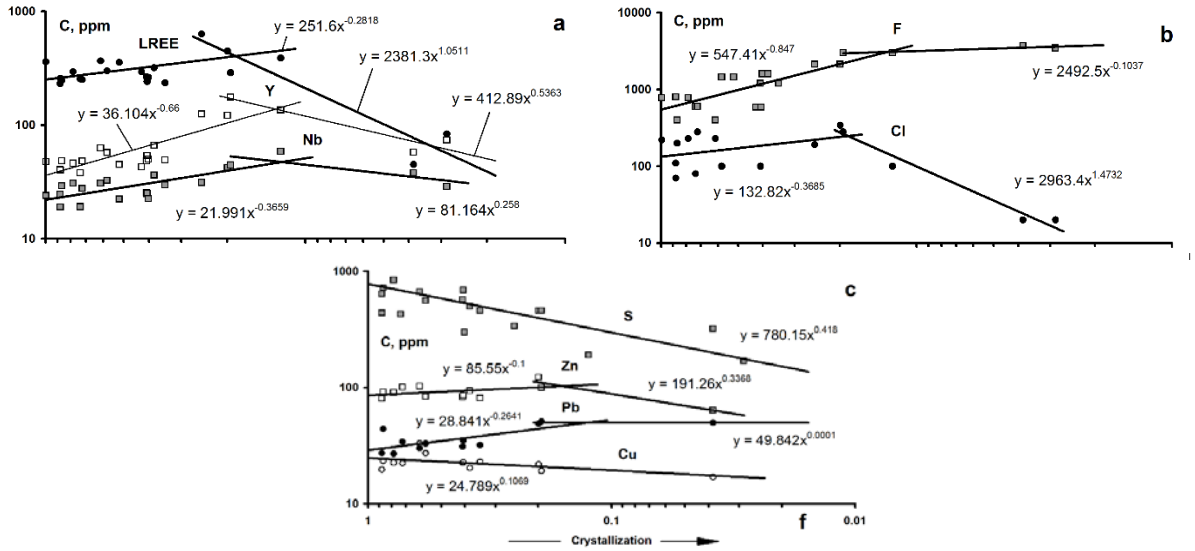

Fig. 5. LREE, Y, Nb, Zn, Pb, Cu, S, Cl and F concentrations in Korosten pluton granitoids vs. *f*

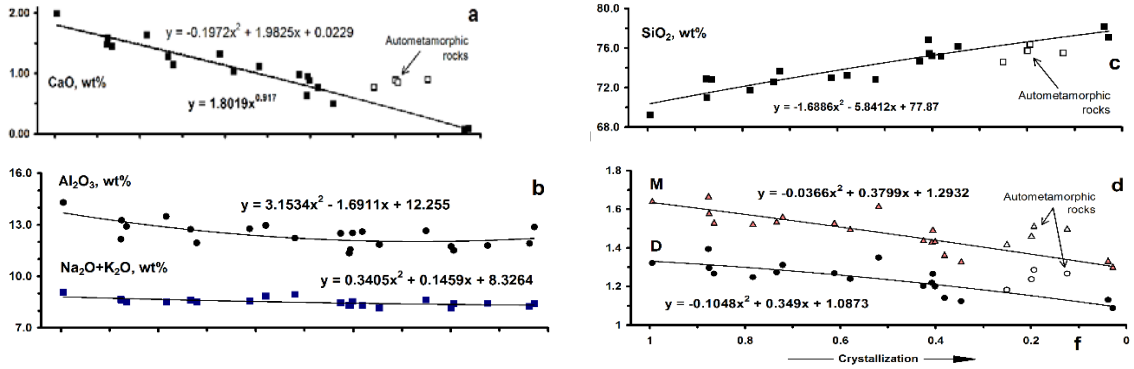

Fig. 6. Selected major elements concentrations and values of M and D bulk composition parameters in Korosten pluton granitoids vs. *f*

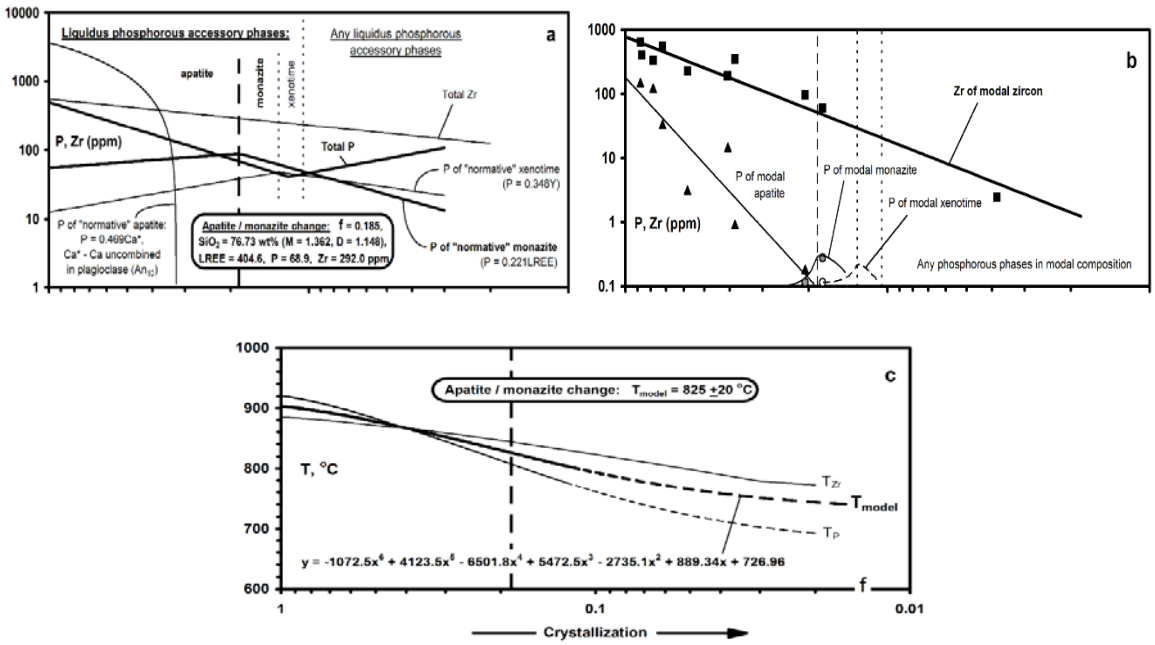

Fig. 7. Evolution of liquidus accessory phases assemblage during the crystallization in magma chamber according to the results of geochemical modelling (a) and modal composition of rocks (b). The estimations of melt composition and temperature in apatite/monazite replacement point are shown on plots (a) and (c) respectively. T_{Zr} and T_P are calculated according to zircon and apatite solubility equations. T_{model} estimated as average of T_{Zr} and T_P in range of f from 1 to 0,185 and extrapolated to f – 0,02. See text for equations and references

Discussion. Elaborated geochemical model establish the key role of fractional crystallization in the Korosten pluton granitoids formation. It indicates the saturation of the initial rapakivi granite melt in both zircon and apatite as well as the

latest differentiates in monazite or xenotime. Some important parameters of magmatic evolution are estimated on this basis. These parameters include: (1) total pressure (P_{total}) of initial melt generation level (P_{total} ~6.3 kbar); (2) temperature of the initial melt (T_{model} = 900°C) and its decrease during the magma differentiation (total range: 900-720^{0}C); (3) water content in the initial melt (H_2O_{model} = $C_0^{H_2O}$ = 2.36 wt%) as well as water content during further magmatic evolution up to the moment of aqueous metal-bearing fluid extraction from the latest differentiates (H_2O_{model} = 10.77 wt%). Finally, the ability of the granitic magma to be the source of high-temperature ore-bearing fluids is demonstrated.

The evaluations obtained are in a good agreement with P values and water content estimations reported by [40] for initial melt of Fennoscandian rapakivi batholiths (P = 5-6 kbar, H_2O = 2.5 wt%). The only differences are in maximum T values reported in this paper (900 and 780°C respectively). In general, it is in order, because zircon, apatite and monazite saturation temperatures are consistent with the residual melts temperatures at the moment of their partition off the solid phase in magma chamber during initial melt fractional crystallization. Therefore, T_{model} is the maximum magma temperature. However, higher T (T_{model}) values obtained in this work could be caused by partly inherited (relict) origin of zircon and apatite. Inherited accessory minerals concentrations must be taken into account in further saturation temperatures evaluations.

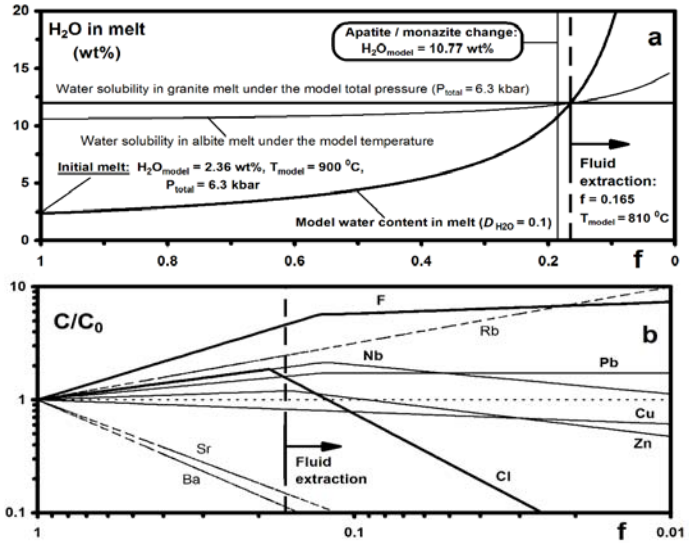

Fig. 8. Conditions of the water-fluid extraction from the melt (a) estimated by assuming Rayleigh fractionation for D_{H2O}=0,1. Water content (H_2O_{model}) in apatite/monazite change point were calculated from T_{model} and D bulk composition parameter values according to monazite solubility equation. Inversion in C/C_0 curves (b) demonstrates the enrichment of water-fluid with Cl, F and ore elements (Zn, Nb, Pb etc.). Similar curves for Sr, Ba and Rb show the low (Sr+Ba)/Rb ratio in fluid. See text for equations and references

In addition, our data must be compared with determination of trace elements and all volatile components content in melt inclusions reported by [7, 15, 25] for pegmatites of the Korosten pluton region. Reported in [15] precise determinations constitute the most correct direct information about the pegmatite melt composition (H_2O = 7 wt%, F = 5.1 wt%, Cl = 0.3 wt%, enrichment in Li, Rb, Cs, Sn, Nb, U, Th and depletion in Ti, P, Zr, Sr, Ba, REE). This data lies in agreement with our model evaluations for the water, other volatile and trace elements content in the latest differentiates of Korosten granitic magma.

Conclusions. (1) Some important parameters of magmatic evolution were estimated for the Korosten pluton granitoids on a basis of geochemical modelling. Model evaluations are in a good agreement with authentic data independently obtained for Korosten pluton and similar rapakivi granite complexes by other researchers.

(2) Not only whole-rock but equilibrated widespread accessory minerals assemblages (zircon+apatite, zircon+monazite etc.) trace elements geochemistry investigations are necessary to increase modelling procedure precision [26, 34, 37]. Also the inherited accessory minerals concentrations must be taken into account in further saturation temperatures evaluations.

(3) Similar geochemical modelling may serve as a powerful tool for other granitoid complexes investigations and economic mineralization prospecting [42, 55].

Authors consider results published in this paper to be preliminary. Reliability enhancement requires involvement of significantly larger amount of geochemical data, which accounts for all major rock types of KP.

Acknowledgements. This work was supported by the Scientific Research Department of the Taras Shevchenko National University of Kiev throughout grant 0116U004784. The authors thank V.G.Molyavko for numerous consultations and sincere interest in this work as well as A.V. Andreev and V.V. Zagorodny for the significant assistance in analytical investigations.

Список використаних джерел

1. Анортозит-рапакивигранитная формация Восточно-Европейской платформы : монография / Д. А. Великославинский, А. П. Биркис, О А. Богатиков и др. – Л. : Наука, 1978. – 296 с.

2. Антипин В.С.Коэффициенты распределения редких элементов в магматических породах : монография / В. С. Антипин, В. И. Коваленко, И. Д. Рябчиков. – М. : Наука, 1984. – 251 с.

3. Артеменко Г.В. Эволюция кислого магматизма в зеленокаменных поясах Украинского щита и Воронежского кристаллического массива / Г. В Артеменко // Минералог. журн. – 1997. – 19. – № 2. – С. 52–59.

4. Богатиков О.А. Магматические горные породы. Кислые и средние породы /О. А. Богатиков, С. В. Богданова, А. М. Борсук и др. – М. : Наука, 1987. – 374 с.

5. Бухарев В.П. Эволюция докембрийского магматизма западной части Украинского щита / В. П. Бухарев. – К. : Наук. думка. – 1992. – 152 с.

6. Верхогляд В.М. Возрастные этапы магматизма Коростенского плутона / В.М. Верхогляд // Геохимия и рудообразование. – 1995. – Вып. 21. – С. 34–47.

7. Возняк Д.К. Фізико-хімічні умови формування та особливості локалізації заноришових пегматитів Волині (Український щит) / Д. К. Возняк, В. І. Павлишин // Мінералог. журнал. – 2008. – № 1, Т. 30. – С. 5–20.

8. Геохронология раннего докембрия Украинского щита. Протерозой. / Н. П Щербак, Г. В. Артеменко, И. М. Лесная и др. – Киев : Наук. думка. – 2008. – 240 с.

9. Гранитоиды Украинского щита: петрохимия, геохимия, рудоносность: Справочник / К. Е. Есипчук, В. И. Орса, И. Б. Щербаков, и др. – Киев : Наук. думка, 1993. – 231 с.

10. Гранитоидные формации Украинского щита / И. Б. Щербаков, К. Е. Есипчук, В. И. Орса и др. – Киев : Наук. думка, 1984. – 191 с.

11. Довбуш Т.И. Результаты изучения докембрийских пород западной части Украинского щита Sm-Nd изотопным методом / Т. И. Довбуш, В. М. Скобелев, Л. М. Степанюк // Минералог. журн. – 2000. – Вып. 22, № 2/3. – С. 132–142.

12.Есипчук К.Е. Петролого-геохимические основы формационного анализа гранитоидов докембрия / К. Е. Есипчук. – Киев : Наук. думка, 1988. – 263 с.

13. Зінченко О.В. Новий прояв топаз-цинвальдитових гранітів в Коростенському плутоні / О. В. Зінченко, І. І. Лазарева // Геологія і магматизм докембрію Українського щита. Зб. наук. праць ІГМР НАН України. – К., 2000. – С. 85–87.

14. Ильченко Т.В. Скоростная модель земной коры и верхов мантии Коростенского плутона (Украинский щит) и ее геологическая интерпретация (по профилю ГСЗ Шепетовка – Чернигов) / Т. В. Ильченко, В. П. Бухарев // Геофиз. журн. – 2001. – Т. 23, № 3. – С. 72–82.

15. Коваленко В.И. Магма пегматитов Волыни: состав и параметры кристаллизации по данным изучения включений минералообразующих сред / В. И. Коваленко и др. // Петрология. – 1996. – Т. 4, № 3. – С. 295–309.

16. Костенко М.М. Глибинна будова земної кори північно-західної частини Українського щита вздовж геотрансекту євробридж-97 за результатами комплексної інтерпретації геолого-геофізичних даних. Стаття 1. Аналіз існуючих моделей будови земної кори / М. М. Костенко, В. І. Трегубенко, С. Г. Лоницька // Мінеральні ресурси України. – 2011. – № 1. – С. 20–29.

17. Кривовичев В.Г. Геохимическая модель формирования редкометалльных гранитных пегматитов / В. Г. Кривовичев // Записки ВМО. – 1989. – Ч. 118. – Вып. 4. –С. 1–12.

18. Личак И.Л. Петрология Коростенского плутона / И. Л. Личак. – Киев : Наук. думка, 1983. – 284 с.

19. Металиди С.В. Сущано-Пержанская зона (геология, минералогия, рудоносность): монография / С. В. Металиди, С. В. Нечаев. – Киев : Наук. думка, 1983. – 135 с.

20. Митрохин О.В. Петрографічний склад комплексів анортозит-рапаківігранітної формації / О. В. Митрохин // Вісн. Київ. нац. ун-ту. Геологія. – 2008. – Вип. 45. – С. 62–66.

21. Митрохин А.В. Полибарическая кристаллизация анортозитов Коростенского плутона (Украинский щит) / А. В. Митрохин, С.В. Богданова, Л. В. Шумлянский // Мінералог. журн. – 2008. – Т. 30, № 2. – С. 36–56.

22. Митрохин А.В. Петрология Малинского массива рапакиви (Коростенский плутон) / А. В. Митрохин, С. В. Богданова, Е. В. Билан // Мінералог. журн. -2009. – Т. 31, № 2. – С. 66–81.

23. Митрохин О.В. Анортозит-рапаківігранітна формація Українського щита: автореф. дис. … докт. геол. наук: спец. 04.00.01 / О. В. Митрохин; [Київ. нац. ун-т ім. Тараса Шевченка]. – К., 2011. – 36 с.

24. Нечаев С.В. Металлогения раннего докембрия и рифея-протерозоя Украинского щита / С. В. Нечаев // Минералог. журн. – 1998. – Вып. 20. – С. 88–99.

25. Оксифлюоцерит (Се) камерних пегматитів Волині (Український щит). / Д. К. Возняк, В. М. Бельський, О. А. Вишневський та ін. // Мінералог. журн. – 2017. – Т. 39, № 3. – С. 3–16.

26. Петрологический анализ геохимии акцессорных цирконов и апатитов из гранитоидов Роховецкой интрузии (Словакия) // С. Е Шнюков, Й. Гатар, А. В. Андреев и др. // Геолог. журн. – 1993. – № 1. – С. 30–41.

27. Петрология, геохимия и рудоносность интрузивных гранитоидов Украинского щита : монография / К. Е. Есипчук, Е. М. Шеремет, О. В. Зинченко и др. – Киев : Наук. думка, 1990. – 236 с.

28.Пономаренко А.Н. Геохронология и геодинамика палеопротерозоя Украинского щита. / А. Н. Пономаренко, Л. М. Степанюк, Л. В. Шумлянский // Минералог. журн. – 2014. – 36, № 2. – С. 48–60.

29. Рябчиков И.Д. Термодинамический анализ поведения малых элементов при кристаллизации силикатных расплавов : монография / И. Д. Рябчиков. – М. : Наука, 1965. – 120 с.

30. Рябчиков И.Д. Термодинамика флюидной фазы гранитоидных магм : монография / И. Д. Рябчиков – М. : Наука, 1975. – 232 с.

31. Соболев В.С. Петрология восточной части сложного Коростенского плутона / В. С. Соболев // Учен. зап. Львовск. ун-та. Геология. – 1947. – Вып. 5. – С. 1–139.

32. Уран-свинцевий вік жильних гранітоїдів Середнього Побужжя / Л. М. Степанюк, О. В. Грінченко, В. М. Загнітко та ін. // Допов. НАН України. – 1996. – № 11. – С. 129–133.

33. U-PB ізотопний вік цирконів з гібридних порід Коростенського анортозит-рапаківігранітного плутону. / О. Білан, О. Митрохин, Л. Шумлянський та ін. // Вісн. Київ. нац. ун-ту. Геологія. – 2016. – Вип. 74, № 3. – С. 6–10.

34. Шнюков С.Є. Геохимия "сквозных" сосуществующих акцессорных минералов и ее роль в исследовании эндо- и экзогенных геологических процессов / С. Е. Шнюков, А. К. Чебуркин, А. В. Андреев // Геолог. журн. – 1989. – Т. 49, № 2. – С. 107–114.

35. Шнюков С.Е. Геохимические модели эволюции магматических систем и земной коры: потенциальный источник петрофизической и рудогенетической информации / С. Е. Шнюков // Геофизический журнал. – 2002. – Т. 24, № 6. – С. 201–219.

36. Шнюков С.Є. Геохімічне моделювання в дослідженні генетичного зв'язку магматичних комплексів та просторово асоціюючих з ними гідротермально-метасоматичних рудних родовищ / С. Є. Шнюков, І. І. Лазарева // Зб. наук. праць УкрДГРІ. – 2002. – № 1. – С. 128–143.

37. Шнюков С.Є. Наскрізні акцесорні мінерали в геохімічному моделюванні магматичних процесів / С. Є. Шнюков // Зб. наук. праць УкрДГРІ. – 2001. – № 1–2. – С. 41–53.

38. Allegre C.J. Quantitative models of trace element behaviour in magmatic processes / C. J. Allegre, J. F. Minster // Earth and Planetary Science Letters. – 1978. – V. 38. – P. 1–25.

39. Dovbush, T.I. Some remarks on the originof the Korosten anorthosite–rapakivi granite complex as basedon isotope data / T. I. Dovbush, V. M. Skobelev // Geophysical Journal. – 2000. – V. 22. – P. 84–85.

40. Eklund O. The origin of rapakivi texture by sub-isothermal decompression / O. Eklund, A. D. Shebanov // Precambrian Research. – 1999. – V. 95. – P. 129–146.

41. Gast P.W. Trace element fractionation and the origin of tholeitic and alkaline magma types / P. W. Gast // Geochim. et Cosmochim. Acta. – 1968. – V. 32. – P. 1057–1086.

42. Gavryliv L. Geochemical behavior of major and trace elements during magma evolution process in Bodie Hills Volcanic Field, Nevada / L. Gavryliv, S. Shnyukov, I. Lazareva // XV-th International Conference "Theoretical and Applied Aspects" (May 10–13, 2016, Kiev, Ukraine). – Режим доступу: http://www.earthdoc.org/publication/publicationdetails/?publication=84616

43. Geochronological constraints on the emplacement history of an anorthosite-rapakivi granite suite: U-Pb zircon and baddeleyite study of the Korosten complex, Ukraine / Yu. V. Amelin, L. M. Heaman, V. M. Verchogliad, V.M. Skobelev // Contrib. Mineral. Petrol. – 1994. – V. 116. – P. 411–419.

44. Greenland L.P. An equation for trace element distribution during magmatic crystallization / L. P. Greenland // Am. Miner. – 1970. – V. 55. – P. 455–465.

45. Harrison T.M. The behavior of apatite during crustal anatexis: Equilibrium and kinetic considerations / T. M. Harrison, E. B. Watson // Geochim. et Cosmochim. – 1984. – Acta 48 – P. 1467–1477.

46. Hertogen J. Calculations of trace element fractionation during partial melting / J. Hertogen, R. Gijbels // Geochim. et Cosmochim. –1976. – Acta 40. – P. 313–322.

47. Maximum and minimum water contents of granitic melts generated in the crust: a revaluation and implications. / F. Holtz, W. Johannes, N. Tamic, H. Behrens // Lithos. – 2001. – V. 56. – P. 1–14.

48. McMillan P.F. Water solubility in aluminosilicate melts. Contrib. Mineral / P. F. McMillan, J. R. Holloway // Petrol. –1987. – 97. – P. 320–332.

49. Montel J.M. A model for monazite/melt equilibrium and application to the generation of granitic magmas / J. M. Montel // Chemical Geology. – 1993. – V. 110. – P. 127–145.

50. Neumann H. Trace element variation during fractional crystallisation as calculated from the distribution law / H. Neumann, J. Mead, C. J. Vitaliano // GCA. – 1954. – № 6. – P. 90–99.

51.Pressure effects, kinetics, and rheology of anorthositic and related magmas. / J. Longhi, M. S. Fram, J. Vander Auwera, J. N. Montieth // Am. Mineral. – 1993. – V. 78. – P.1016–1030.

52. Shaw D.M. Trace element fractionation during anatexis / D.M. Shaw // Geochim. et Cosmochim. – 1970. – Acta 34. – P. 237–243.

53. Soesoo A. Fractional crystallization of mantle-derived melts as a mechanism for some I-type granite petrogenesis: an example from Lachlan Fold Belt, Australia. / A. Soesoo // J. Geol. Soc. London. – 2000. – V. 157. – P. 135–149.

54. The 1.80-1.74-Ga gabbro-anorthosite-rapakivi Korosten Pluton in the Ukrainian Shield: a 3-D geophysical reconstruction of the deep structure / S. V. Bogdanova, I. K. Pashkevich, V. B. Buryanov et al. // Tectonophysics. – 2004. – V. 381. – P. 5–27.

55. Volcanoes of Antarctica as object of geological and ecological research at an example of Deception Island / I. Lazareva, S. Shnyukov, E. Hlon et al. // Materials of XI Unternational Scientific Conference "Monitoring of Geological Processes and Ecological Condition of the Enviroment" (October 11–14, 2017, Kyiv, Ukraine).

56. Watson E.B. Zircon saturation revisited: temperature and composition effects in a variety of crustal magma types / E. B. Watson, T. M. Harrison // Earth and Planetary Science Letters. – 1983. – V. 64. – P. 295–304.

References

1. Velikoslavinsky, D.A., Birkis, A.P., Bogatikov, O.A., Bukharev, V.P., Velikoslavinsky, S.D., Gordienko, L.I., Zinchenko, O.V., Kivisilla, Ya.Ya., Kirs, Yu.E., Kononov, Yu.V., Levitsky, Yu.F., Niin, M.I., Puura, V.A., Khvorov, M.I., Shustova, L.E. (1978). The anorthosite-rapakivi granite formation of the East European platform. Leningrad: Nauka Press, 296. [in Russian].

2. Antipin, V.S., Kovalenko, V.I., Ryabchikov, I.D. (1984). Distribution coefficients of rare elements in magmatic rocks. Moscow: Nauka Press, 251. [in Russian].

3. Artemenko, G.V. (1997). Granitoidemagmatism evolution of greenstone belts of the Ukrainian Shield and adjacent Voronezh crystalline massife. Mineralogical Journal, 19, 4, 89-92. [in Russian].

4. Bogatikov, O.A., Bogdanova, S.V., Borsuk, A.M. et al. (1987). Magmatic rocks: Vol. 4. Acid and mediosilicic rocks. Moscow: Nauka Press, 374. [in Russian].

5. Bukharev, V.P. (1992). Evolution of precambrian magmatism of western part of Ukrainian Shield. K.: Nauk. dumka, 152. [in Russian].
6. Verchogliad, V.M. (1995). Age stages of magmatic processes of the Korosten pluton. Geochemistry and ore formation, 21, 34-47. [in Russian].
7. Voznyak, D. K., Pavlishin, V.I. (2008). Physical-chemical condition of formation and localization features of miarolitic (chamber) pegmatites of Volyn (Ukrainian Shield). Min. Journ., 1, 30, 5-20. [in Ukrainian].
8. Sherbak, N.P., Artemenko, G.V., Lesnaya, I.M. et al. (2008). Geochronology of early Precambrian Ukrainian Shield. Proterozoic. Kiev: Nauk. dumka, 240. [in Russian].
9. Esipchuk, K.E., Orsa, V.I., Scherbakov, I.B., Sheremet, E.M., Skobelev, V.M., Ryabokon, V.V., Galitsky, L.S., Panov, B.S., Yushin, A.A., Bochay, L.V., Golub, E.N., Demyanenko, V.V., Buchinskaya, K.M., Sveshnikov, K.I., Sukhorukov, Yu.T., Scherbak, D.N., Osadchy, V.K., Piya, Yu.K., Samchuk, A.I., Kushnir, A.S., Andreev, A.V., Cheburkin, A.K. (1993). Granitoids of the Ukrainian Shield: petrochemistry, geochemistry and ore deposites (reference book). Kiev: Naukova Dumka, 231. [in Russian].
10. Scherbakov, I.B., Esipchuk, K.E., Orsa, V.I., Usenko, I.S., Bartnitsky, E.N., Golub, E.N., Gorlitsky, B.A., Kirillov, S.P., Zabiyaka, L.I., Tsarovsky, I.D., Osadchy, V.K. (1984). Granitoids formations of the Ukrainian Shield. Kiev: Naukova Dumka, 191. [in Russian].
11. Dovbush, T.I., Skobelev, V.M., Stepaniuk, L.M. (2000). Results of Sm-Nd investigation of the Precambrian rocks of western parts of the Ukrainian Shield. Mineralogical Journal, 22, 2/3, 132-142. [in Russian].
12. Esipchuk, K.E. (1988). Petrological and geochemical fundamentals of formational analysis of Precambrian granitoids. Kiev: Naukova Dumka, 263. [in Russian].
13. Zinchenko, O.V., Lazareva, I.I. (2000). New manifestation of topaz-zinnvaldite granites in the Korosten pluton. In: Geology and magmatism of Precambrian of the Ukrainian Shield. Kiev, 185-187. [in Ukrainian].
14. Ilchenko, T.V., Buharev, V.P. (2001). Velocity model of earth crust and upper mantle of Korosten Pluton (Ukrainian Shield) and its geological interpretation (along GSZ Shepetovka – Chernihiv profile). Geophysical Journal, 3, 23, 72-82. [in Russian].
15. Kovalenko, V.I., Tsareva, G.M., Naumov, V.B., Hervig, R., Newman, S. (1996). Magma of the Volyn pegmatites: composition and crystallization parameters obtained by mineralogical inclusions investigations. Petrologia, 4, 3, 295-309. [in Russian].
16. Kostenko, M.M., Tregubenko, V.I., Lonycka, S.G. (2011). Deep structure of northwestern part of Ukrainian Shield's earth crust along geotransect eurobridge-87 by results of complex interpretation of geological-geophysical data. Article 1. Analysis of existing models of earth crust structure. Mineral resources of Ukraine, 1, 20-29. [in Ukrainian]
17. Krivovichev, V.G. (1989). Geochemical model for rare-metal granite pegmatites formation. Zapisky Vserossiyskogo Mineralogicheskogo Obschestva, 4, 1-12. [in Russian].
18. Lichak, I.L. (1983). Petrology of the Korosten Pluton. Kiev: Naukova Dumka, 284. (in Russian).
19. Metalidi, S.V., Nechaev, S.V. (1983). Suschano-Perga area (geology, mineralogy and ore deposits). Kiev: Naukova Dumka, 135. [in Russian].
20. Mytrohyn, O.V. (2008). Anorthosite-rapakivi-granite association complexes petrographic composition. Visnyk of Taras Shevchenko National University of Kyiv. Geology, 45, 62-66. [in Ukrainian].
21. Mytrohyn, O.V., Bogdanova, S.V, Shumlyanskiy, L.V. (2008). Polybaric crystallization of Korosten pluton anorthosites (Ukrainian Shield). Mineralogical Journal, 30, 2 36-56. [in Russian].
22. Mytrohyn, O.V., Bogdanova, S.V., Bilan, E.V. (2009). Petrology of Malin rapakivi massive (Korosten.pluton). Mineralogical Journal, 31, 2, 66-81. [in Russian].
23. Mitrokhin, O. V. (2011). Anorthosite-rapakiva granite association of Ukrainian Shield: Autoref. Dis. … doc. of Geol. Sci.: spec. 04.00.01. Taras Schevchenko National University of Kyiv. K., 36. [in Ukrainian].
24. Nechaev, S.V. (1998). Early Precambrian and Riphean-Phanerozoic metallogeny of the Ukrainian Shield. Mineralogical Journal, 20, 88-99. [in Russian].
25. Voznyak, D.K., Belskyy, V.M., Vyshnevskyy, O.A., Ilchenko, K.O., Kurylo S.I. (2017) Oxyfluocerite of chamber pegmatites of Volyn (the Ukrainian Shiled). Mineralogical Journal, 3, 39, 3-16. [in Ukrainian]
26. Shnyukov, S.E., Hatar, J., Andreev, A.V., Gregush, J., Cheburkin, A.K., Savenok, S.P. (1993). Petrological analysis of accessory zircon and apatite geochemistry in granitoids of Rochovce intrusion (Slovakia). Geological Journal, 1, 30-41. [in Russian].
27. Esipchuk, K.E., Sheremet, E.M., Zinchenko, O.V., Bobrov, A.B., Borko, V.N., Bukharev, S.V., Vasilchenko, V.V., Verchogliad, V.M., Golub, E.N., Demyanenko, V.V., Zhebrovskaya, E.I., Orsa, V.I., Panov, B.S., Razdorozhny, V.F., Sveshnikov, K.I., Skobelev, V.M., Scherbak, D.N. (1990). Petrology, geochemistry and ore mineralization of intrusive granitoids of Ukrainian Shield. Kiev: Naukova Dumka, 236. [in Russian].
28. Ponomarenko, A.N., Stepanuyk, L.M., Shumlyanskiy, L.V. (2014). Geochronology and geodynamics of Paleoproterozoic Ukrainian Shield. Mineralogical journal, 36, 2, 48-60. [in Russian].
29. Ryabchikov, I.D. (1965). Thermodynamic analysis of trace elements behavior during the silicate meltcrystallisation. Moscow: Nauka, 120. [in Russian].
30. Ryabchikov, I.D. (1975). Thermodynamics of the fluid phase in granitoid magmas Moscow: Nauka, 232. [in Russian].
31. Sobolev, V.S. (1947). Petrology of eastern part of the complex Korosten pluton. Science Notes of Lviv University 6, 5, 1-139. [in Russian].
32. Stepaniuk, L.M., Grinchenko, O.V., Zagnitko, V.M., Bartnitsky, E.M. (1996). Isotopical investigation of vein granitoides of Middle Pobuzhie region, Ukrainian Shield. Papers of National Academy of Sciences of Ukraine, 11, 129-133 [in Ukrainian].
33. Bilan, O., Mitrokhin, O., Shumlyanskiy, L., Zagorodniy, V. (2016). U-Pb age of zircons from hybrid rocks of Korosten anorthosite-rapakive granite pluton. Visnyk of Taras Shevchenko National University of Kyiv. Geology, 7, 74, 3, 6-10. [in Ukrainian].
34. Shnyukov, S.E., Cheburkin, A.K., Andreev, A.V. (1989). Geochemistry of wide-spread coexisting accessory minerals and their role in investigation of endogenetic and exogenetic processes. Geological Journal, 2, 107-114. [in Russian].
35. Shnyukov, S.E. (2002). Geochemical models of magmatic systems and earth's crust evolution: potential source of petrophysical and ore-genetical information. Geophysical journal, 24, 6, 201-219. [in Russian].
36. Shnyukov, S.E., Lazareva, I.I. (2002). Geochemical modeling in research of genetic connection of magmatic complexes and spatially associated hydrothermal-metaspmatic ore deposits. Zbirnuk naukovih prats UkrDGRI, 1, 128-143. [In Ukrainian].
37. Shnyukov, S.E. (2001). Ubiquitous accessory minerals in geochemical modeling of magmatic processes. Zbirnik naukovih prats UkrDGRI, 1-2, 41-53. [In Ukrainian].
38. Allegre, C.J., Minster, J.F. (1978). Quantitative models of trace element behaviour in magmatic processes. Earth and Planetary Science Letters, 38, 1-25.
39. Dovbush, T.I., Skobelev, V.M. (2000). Some remarks on the originof the Korosten anorthosite–rapakivi granite complex as basedon isotope data. Geophysical Journal, 22, 84–85.
40. Eklund, O., Shebanov, A.D. (1999). The origin of rapakivi texture by sub-isothermal decompression. Precambrian Research, 95, 129-146.
41. Gast, P.W. (1968). Trace element fractionation and the origin of tholeitic and alkaline magma types. Geochim. et Cosmochim. Acta, 32, 1057-1086.
42. Gavryliv, L. Shnyukov, S., Lazareva, I. (2016). Geochemical behavior of major and trace elements during magma evolution process in Bodie Hills Volcanic Field, Nevada. XV-th International Conference of Geoinformatocs "Theoretical and Applied Aspects" (May 10-13, 2016, Kiev, Ukraine). URL: http://www.earthdoc.org/publication/publicationdetails/?publication=84616
43. Amelin, Yu.V., Heaman, L.M., Verchogliad, V.M., Skobelev, V.M. (1994). Geochronological constraints on the emplacement history of an anorthosite-rapakivi granite suite: U-Pb zircon and baddeleyite study of the Korosten complex, Ukraine. Contrib. Mineral. Petrol., 116, 411-419.
44. Greenland, L.P. (1970). An equation for trace element distribution during magmatic crystallization. Am. Miner., 55, 455-465.
45. Harrison, T.M., Watson, E.B. (1984). The behavior of apatite during crustal anatexis: Equilibrium and kinetic considerations. Geochim. et Cosmochim., Acta, 48, 1467-1477.
46. Hertogen, J., Gijbels, R. (1976). Calculations of trace element fractionation during partial melting. Geochim. et Cosmochim., Acta, 40, 313-322.
47. Holtz, F. Johannes, W., Tamic, N., Behrens, H. (2001). Maximum and minimum water contents of granitic melts generated in the crust: a revaluation and implications. Lithos, 56, 1–14.
48. McMillan, P.F., Holloway, J.R. (1987). Water solubility in aluminosilicate melts. Contrib. Mineral. Petrol., 97, 320-332.
49. Montel, J.M. (1993). A model for monazite/melt equilibrium and application to the generation of granitic magmas. Chemical Geology, 110, 127-145.
50. Neumann, H., Mead, J., Vitaliano, C.J. (1954). Trace element variation during fractional crystallisation as calculated from the distribution law. GCA, 6, 90-99.
51. Longhi, J. Fram, M.S., Vander Auwera, J., Montieth, J.N. (1993). Pressure effects, kinetics, and rheology of anorthositic and related magmas. Am. Mineral, 78, 1016-1030.
52. Shaw, D.M. (1970). Trace element fractionation during anatexis. Geochim. et Cosmochim. Acta, 34, 237-243.
53. Soesoo, A. (2000). Fractional crystallization of mantle - derived melts as a mechanism for some I - type granite petrogenesis: an example from Lachlan Fold Belt, Australia. J. Geol. Soc. London. 157, 135–149.
54. Bogdanova, S.V., Pashkevich, I.K., Buryanov, V.B. et al. (2004). The 1.80-1.74-Ga gabbro-anorthosite-rapakivi Korosten Pluton in the Ukrainian Shield: a 3-D geophysical reconstruction of the deep structure. Tectonophysics, 381, 5-27.
55. Lazareva, I., Shnyukov, S., Hlon, E., Aleksieienko, A., Morozenko, V., Gavryliv, L. (2017). Volcanoes of Antarctica as object of geological and ecological research at an example of Deception Island. Materials of XI Unternational Scientific Conference "Monitoring of Geological Processes and Ecological Condition of the Enviroment" (October 11-14, 2017, Kyiv, Ukraine).
56. Watson, E.B., Harrison, T.M. (1983). Zircon saturation revisited: temperature and composition effects in a variety of crustal magma types. Earth and Planetary Science Letters, 64, 295-304.

Надійшла до редколегії 06.11.17

С. Шнюков, д-р геол. наук, доц.
E-mail: shnyukov@mail.univ.kiev.ua
І. Лазарєва, канд. геол. наук, доц.
E-mail: lazareva@mail.univ.kiev.ua
О. Зінченко, канд. геол. наук, доц.
О. Хлонь, інж.
E-mail: khlon@univ.kiev.ua
Л. Гаврилів, асп.
E-mail: liubomyr.gavryliv@gmail.com
А. Алексєєнко, асп.
E-mail: scr315@gmail.com
Київський національний університет імені Тараса Шевченка
ННІ "Інститут геології", вул. Васильківська 90, м. Київ, 03022, Україна

ГЕОХІМІЧНА МОДЕЛЬ МАГМАТИЧНОЇ ЭВОЛЮЦІЇ ГРАНІТОЇДІВ КОРОСТЕНСЬКОГО ПЛУТОНУ (УКРАЇНСЬКИЙ ЩИТ): ПЕТРОГЕНЕТИЧНІ АСПЕКТИ І ГЕНЕЗИС РУДНОЇ МІНЕРАЛІЗАЦІЇ В МЕТАСОМАТИЧНИХ ЗОНАХ

Було вивчено попередній набір геохімічних даних для гранітоїдів (рапаківі, граніт-порфіри та жильні граніти) Коростенського анортозит-рапаківігранітного плутону (КП) Українського щита. Дані щодо мікроелементного складу гранітоїдів достатньо близько апроксимуються моделлю фракційної кристалізації Релея. Для Rb встановлено типову несумісну поведінку з постійним комбінованим коефіцієнтом розподілу (D_{Rb} = 0,5), що дозволило провести розрахунок значення f (масової частки рідкої фази в магматичній камері) для кожного типу гранітоїдів (порції залишкового розплаву) приймаючи мінімальний вміст елемента в гранітоїдах (169 ppm) за його вміст у материнському розплаві (C_0^{Rb}). Залежність концентрацій від f для мікро- (включаючи P, Ti, S, Cl, F, Ca) і петрогенних елементів апроксимовані рівняннями виду $C=C_0\ f^{D-1}$ або поліноміальними, відповідно. Одержаний набір рівнянь є ідеалізованою моделлю поведінки елементів, яка ілюструє характер еволюції розплаву в процесі фракційної кристалізації: виснаження Ba, Sr, Ti, Zr, P, S; збагачення Th, Ga; інверсію поведінки LREE, Y, F, Cl, Nb, Zn и Pb. Монотонне зниження концентрації Zr і P вказує на насичення розплаву цирконом та апатитом, що дозволило провести розрахунок модельних температур (T_{model}) користуючись експериментальними рівняннями розчинності циркону і апатиту в силікатних розплавах, а також отримати поліноміальне рівняння залежності T_{model} від f (діапазон T_{model}: 900-720°C). Вміст води у розплаві для моменту заміни апатиту монацитом у продуктах кристалізації (інверсія поведінки LREE; f = 0,185) розраховано з рівняння розчинності монациту. Оцінку вмісту води у вихідному розплаві (C_0^{H2O}=2,36 wt%) і тиску в магматичній камері (P_{total} ~ 6,3 kbar) проведено, припускаючи, що D_{H2O} = 0,1. Відокремлення водного флюїду внаслідок насичення системи водою, виходячи з розробленої моделі, відбулося при f = 0,165. Синхронна інверсія C/C_0 вказує на збагачення флюїду F, Cl, Nb, Zn, Pb тощо. Дані про склад флюїду відповідають геохімічним даним про склад асоціюючих з КП метасоматично змінених порід, що може свідчити про їх генетичну єдність.

Ключові слова: граніт, рапаківі, мікроелементи, магматична еволюція, апатит, циркон, монацит, ксенотим, розчинність, вода в розплаві, відокремлення флюїду, метасоматити, рудна мінералізація.

С. Шнюков, д-р геол. наук, доц.
E-mail: shnyukov@mail.univ.kiev.ua
И. Лазарева, канд. геол. наук, доц.
E-mail: lazareva@mail.univ.kiev.ua
О. Зинченко, канд. геол. наук, доц.
Е. Хлонь, инж.
E-mail: khlon@univ.kiev.ua
Л. Гаврылив, асп.
E-mail: liubomyr.gavryliv@gmail.com
А. Алексеенко, асп.
E-mail: scr315@gmail.com
Киевский национальный университет имени Тараса Шевченко
УНИ "Институт геологии", ул. Васильковская 90, г. Киев, 03022, Украина

ГЕОХИМИЧЕСКАЯ МОДЕЛЬ МАГМАТИЧЕСКОЙ ЭВОЛЮЦИИ ГРАНИТОИДОВ КОРОСТЕНСКОГО ПЛУТОНА (УКРАИНСКИЙ ЩИТ): ПЕТРОГЕНЕТИЧЕСКИЕ АСПЕКТЫ И ГЕНЕЗИС РУДНОЙ МИНЕРАЛИЗАЦИИ В МЕТАСОМАТИЧЕСКИХ ЗОНАХ

Был изучен предварительный набор геохимических данных для гранитоидов (рапакиви, гранит-порфиры и жильные граниты) Коростенского анортозит-рапакивигранитного плутона (КП) Украинского щита. Данные о микроэлементном составе гранитоидов достаточно близко аппроксимируются моделью фракционной кристаллизации Релея. Для Rb установлено типичное несовместимое поведение с постоянным комбинированным коэффициентом распределения (D^{Rb} = 0,5), что позволило произвести расчет значения f (массовой доли жидкой фазы в магматической камере) для каждого типа гранитоидов (порции остаточного расплава) принимая минимальное содержание элемента в гранитоидах (169 ppm) за его содержание в материнском расплаве (C_0^{Rb}). Зависимости концентраций от f для микро- (включая P, Ti, S, Cl, F, Ca) и петрогенных элементов аппроксимированы уравнениями вида $C=C_0\ f^{D-1}$ или полиномиальными, соответственно. Полученный набор уравнений является идеализированной моделью поведения элементов, которая илюстрирует характер эволюции расплава в процессе фракционной кристаллизации: истощение Ba, Sr, Ti, Zr, P, S; обогащение Th, Ga; инверсию поведения LREE, Y, F, Cl, Nb, Zn и Pb. Монотонное снижение концентрации Zr и P указывает на насыщение расплава цирконом и апатитом, что позволило произвести расчет модельных температур (T_{model}) используя экспериментальные уравнения растворимости циркона и апатита в силикатных расплавах, а также получить полиномиальное уравнение зависимости Tmodel от f (диапазон T_{model}: 900-720°C). Содержание воды в расплаве для момента замены апатита монацитом в продуктах кристаллизации (инверсия поведения LREE; f = 0,185) рассчитано из уравнения растворимости монацита. Оценка содержания воды в исходном гранитном расплаве (C_0^{H2O}=2,36 wt%) и давления в магматической камере (Ptotal ~6,3 kbar) проведена, предполагая, что D_{H2O} = 0,1. Отделение водного флюида вследствие насыщения системы водой, исходя из разработанной модели, произошло при f = 0,165. Синхронная инверсия C/C_0 указывает на обогащение флюида F, Cl, Nb, Zn, Pb и т. д. Данные о составе флюида соответствуют геохимическим данным о составе ассоциирующих с КП метасоматически измененных пород, что может свидетельствовать об их генетическом единстве.

Ключевые слова: гранит, рапакиви, микроэлементы, магматическая эволюция, апатит, циркон, монацит, ксенотим, растворимость, вода в расплаве, отделение флюида, метасоматиты, рудная минерализация.